Athermal Lattice Polymers: A Comparison of RISM Theory and Monte Carlo Simulations

R. H. C. Janssen and E. Nies*

Department of Polymer Technology, Eindhoven University of Technology, P.O. Box 513, 5600 MB Eindhoven, The Netherlands

P. Cifra

Polymer Institute, Slovak Academy of Sciences, 842 36 Bratislava, Slovakia

Received September 17, 1996; Revised Manuscript Received May 5, 1997[⊗]

ABSTRACT: Polymer−RISM theory is applied to study athermal polymeric lattice fluids. The intermolecular segmental distributions and the compressibility equation of state (EoS) have been obtained within the approach for three different intramolecular distribution functions, i.e., the random flight, the non reversal random walk, and an intramolecular distribution obtained from Monte Carlo simulations. Both the intermolecular segmental distributions and the EoS are also compared to Monte Carlo simulations. From the comparison to the simulations it is seen that the polymer−RISM theory is well able to reproduce the intermolecular segmental distributions, but it underestimates the density dependence of the EoS: the EoS is worse than the classical Huggins EoS for the same model, and only for the computer simulated intramolecular distribution we find reasonable agreement between calculated and simulated EoS. The absence of liquidlike ordering effects in a lattice fluid allow us to show to what extent the deviations are due to the incomplete incorporation of excluded volume in the intramolecular distribution functions.

1. Introduction

Equation of state properties of polymeric materials are of great importance in the process industry. They are in principle fully determined by the molecular organization of the material, and therefore, a lot of attention has been paid to the development of molecular based equations of state over the years.[1−9] The most simple polymeric molecules consist of a linear sequence of covalently coupled particles (the segments). The ordering of the particles in the material is then determined by three types of interactions among the particles: repulsive interactions (packing effects), attractive interactions (cohesion), and covalent bonding (chain connectivity).

Classical theories that try to explain the thermal properties from the molecular organization[1−5,10−14] all start from the fundamental statistical mechanical equation, $A_{conf} = -k_B T \ln Q_N$.[15,16] It relates the configurational Helmholtz free energy A_{conf}, a thermodynamic quantity, to the configurational integral Q_N, which probes all molecular configurations that are possible in the polymeric material. Once the Helmholtz free energy is known, all other thermodynamic parameters of the polymeric material follow from well-established thermodynamic relations.[17] Principal difficulty in the approach is the calculation of the configurational integral, Q_N, from the molecular organization of the material. For that purpose the classical approaches adopt approximations resulting in a neglect of local structural correlations. Often, space is discretized such that a segment is captured into a cell[1,2] or a lattice site.[3,4,10] This approximation amounts to a complete[3,4,10] or partial[1,2] neglect of the packing effects that are present in real polymeric liquids. Other approximations regard the effects of the attractive interactions (Bragg−Williams approximation; quasi-chemical approximation)[15,16] and the chain connectivity[11,12] on the structural correlations. Despite these approximations, the models have been quite successful in explaining the thermodynamic behavior of polymeric materials. Comparison to Monte Carlo simulations for the equation of state (EoS)[18] and the liquid−gas[19] and liquid-liquid phase behavior[20−22] of such models has sometimes lead to an almost quantitative agreement. Relatively recent developments along this line of work comprise the generalized-Flory theory[6,23] which incorporates packing effects by generalizing the Flory[11] and Huggins[12] theory to continuum space, and Bawendi and Freed's principally exact solution for the polymeric lattice model.[24,25]

Another line of development toward the thermal properties of polymer liquids originates from liquid state physics.[26−31] In this line of work, one attempts to calculate the structural correlations, i.e., the organization of the molecules in space, as accurately as possible. The models studied within this approach are continuum space models which show liquidlike packing effects caused by the repulsive cores of the particles in the fluid. Principal routes to incorporate the effect of attractive interactions[27,33−38] and chain-connectivity[30,39−41] have been developed, and comparisons to Monte Carlo simulations have been made.[42−44]

Of this line of work, especially the polymer−RISM (PRISM) theory of Curro and Schweizer[39] has proven to be a tractable method to accurately reproduce the structural correlations in continuum polymeric fluids. The (polymer−)RISM theory makes it feasible to predict the intermolecular correlations between segments on different molecules from information of the intramolecular correlations between segments of the same molecule. For simple (rigid) molecules the intramolecular correlations are known in advance, and the RISM theory is quite successful in describing the subtle packing effects in dense liquids induced by the intramolecular structure. For flexible macromolecules, the intramolecular structure is not a priori known but depends on the intermolecular correlations. Hence, a complicated interdependence between inter- and in-

* Author to whom correspondence should be addressed.
[⊗] Abstract published in *Advance ACS Abstracts,* August 1, 1997.

S0024-9297(96)01386-1 CCC: $14.00

tramolecular correlations exists, and in principle, both types of correlations must be calculated self-consistently. The first attempts to establish this self-consistency have been published relatively recently and are still a matter of further investigation.[45−47]

In the initial applications of the PRISM theory, a more simple approach was taken and it was assumed that the intramolecular structure is a priori known.[39] In certain instances this additional approximation turns out to be very reasonable. In particular in a dense pure melt it is known from the ideality hypothesis of Flory[48] that the intramolecular correlations are successfully described by an ideal chain model. However, at low densities the screening of excluded volume interactions becomes less efficient and the intramolecular correlations evolve to those of a self-avoiding random walk.

Once the intramolecular and intermolecular correlations are known, the EoS and other macroscopic material properties can be obtained via formally exact statistical mechanical routes.[26,32] Possible routes to the equation of state are, e.g. the compressibility equation, the energy equation, the virial equation, and the wall equation of state.[49] If the theoretically calculated correlation functions were exact, the equation of state obtained from these different routes would be identical. However, the approximate nature of the PRISM equation and its closures result in so called thermodynamic inconsistencies that make the results depend on the chosen route.[39,50]

In this work we have discretized the polymer−RISM model onto a cubic lattice with a fraction η_m of the available sites filled with linear molecules. Previous integral equation studies for lattice polymers, employing the BGY hierarchy, have been performed by Lipson and co-workers.[51−52] Here, we only consider athermal fluids consisting of molecules without attractive segment−segment interactions.

The objective of our work is 2-fold. First, for a simple nonoverlapping and noninteracting monatomic lattice fluid, all structural correlations are completely absent.[53,54] This implies that the correlations in the case of noninteracting polymeric lattice fluids are only due to the covalent bonding between the segments of the molecules. Thus, by comparison to Monte Carlo simulations, we can investigate the abilities of the polymer−RISM theory to account for chain-connectivity effects on the structural correlations, without the interference of liquidlike packing effects that dominate to a great extent the structural correlations in continuum fluids. A second objective of the work presented here is to make a direct comparison of the polymer−RISM theory to a classical lattice model. For that purpose the compressibility EoS obtained within the polymer−RISM approach is compared to the EoS of the compressible lattice fluid obtained within the Huggins approximation.[12,18] The EoS are also compared to NpT−Monte Carlo simulations.

It should be pointed out that the compressibility route to the equation of state may not be the most accurate route available. Off-lattice studies showed that the compressibility equation of state underestimates the compressibility factor. Other routes to the equation of state also have their deficiencies, although it was demonstrated that for a continuum fluid the wall equation of state produced more accurate results.[50] However, in a lattice study it was shown that the wall equation of state also shows large deficiencies when compared to MC simulation data.[55] This was a good reason for us to examine the compressibility route for the lattice fluids studied in this work.

The rest of this paper is organized as follows. In section 2 the lattice formulation of the polymer−RISM theory is briefly considered, our solution method is outlined, and the compressibility EoS is given. In section 3 the NpT -simulation method is briefly described. In section 4 results for the intermolecular two-particle distribution function $g(l, m, n)$ of a dimeric fluid and of fluids consisting of linear 16- and 30-mers are presented. For the intramolecular two-particle distributions, $\omega(l, m, n)$, which are needed as an input for the calculation of the intermolecular two-particle distributions, $g(l, m, n)$, we have used the random flight (RF) model,[56] the nonreversal random walk model, and intramolecular distributions obtained from MC simulations. The results on the structure are compared to the MC data, and the abilities of the polymer−RISM model to incorporate chain connectivity effects are discussed. The compressibility EoS is compared to the Huggins EoS[12] and to MC data. Concluding remarks are made in section 5.

2. The Discretized Polymer−RISM Equation

2.1. Structural Correlations. Consider N chains that are packed in a volume V discretized by a 3D cubic mesh. The molecules each consist of s segments, numbered from 1 to s, occupying consecutive nearest neighbor sites on the lattice. The chains are flexible in nature. The overall fraction of filled lattice sites η_m, the segmental packing fraction, is given by

$$\eta_m = \frac{Nsv_0}{V} \tag{1}$$

where v_0 is the volume of a lattice site. The chain density can be defined as $\eta = \eta_m/s$.

The molecular organization of a lattice fluid, consisting of flexible polymeric molecules at chain density η, is fully quantified if the inter- and intramolecular two-particle distributions, $g_{ij}(l, m, n)$ and $\omega_{ij}(l, m, n)$, are known. Here, i and j denote respectively the ith and jth segment in a linear molecule ($\{i, j\} \in \{1, s\}$), and (l, m, n) denotes the distance in x, y, and z directions between segments i and j. If $g_{ij}(l, m, n)$ is considered, then i and j belong to two arbitrary but different molecules, and if $\omega_{ij}(l, m, n)$ is considered, then i and j belong to the same molecule. Physically, $\eta_j g_{ij}(l, m, n)$ corresponds to the probability that if the lattice site at (0, 0, 0) is occupied by segment i of a molecule, the lattice site at (l, m, n) is occupied by a jth segment of another molecule. The η_j is the packing fraction of jth segments on the lattice, it is equal to the chain-density η. $\omega_{ij}(l, m, n)$, on the other hand, is the probability of finding segment j at position (l, m, n) and segment i, which belongs to the same molecule, at the origin. Thus, $\omega(l, m, n)$ is a measure of the conformation of a molecule. Chandler and Andersen[30] related the total two-particle correlation function, $h_{ij}(l, m, n)$, defined by

$$h_{ij}(l, m, n) = g_{ij}(l, m, n) - 1 \tag{2}$$

to the direct two-particle correlation function $c_{ij}(l, m, n)$ and the intramolecular two-particle distribution $\omega_{ij}(l, m, n)$ in a manner that bears strong resemblance to the Ornstein−Zernike (OZ) equation for simple fluids.[26] Unfortunately, the RISM theory of Chandler and Andersen becomes intractable for molecules consisting of

many segments. Curro and Schweizer first realized that in the case of ring shaped molecules there is an equivalence of segments within the molecule which permits dropping the segment indices of h_{ij}, c_{ij}, and ω_{ij} and therefore strongly reduces the complexity of the problem.[39] In a later paper they showed that this is also approximately true for long chain-like molecules.[57] Their final result, mapped on the cubic lattice, is[58]

$$h(l, m, n) = \sum_{l',m',n'} \sum_{l'',m'',n''} \omega(l - l', m - m', n - n') c(l' - l'', m' - m'', n' - n'') (\omega(l'', m'', n'') + \eta_m h(l'', m'', n'')) \quad (3)$$

where $\omega(l, m, n)$ is the segment-averaged intramolecular distribution function given by

$$\omega(l, m, n) = \frac{1}{s} \sum_{i=1}^{s} \sum_{j=1}^{s} \omega_{ij}(l, m, n) \quad (4)$$

The $h(l, m, n)$ and $c(l, m, n)$ in eq 3 are the segment-averaged total and direct correlation functions. Equation 3 is the cubic lattice version of Curro and Schweizer's polymer−RISM equation. The $\omega(l, m, n)$ denotes the average number of segments of a chain that will be found on position (l, m, n) from an average segment of the same chain.

The polymer−RISM equation can be solved using an approximate closure equation. In this work we have used the Percus−Yevick closure. It is given by[27]

$$c(l, m, n) = g(l, m, n) (1 - e^{\beta u(l,m,n)}) \quad (5)$$

in which $u(l, m, n)$ is the segmental interaction potential and $\beta = 1/k_B T$. For an athermal fluid in which the polymer segments occupy exactly one lattice site, we have the segment−segment interaction potential

$$u(0, 0, 0) \rightarrow \infty$$

$$u(l, m, n) = 0 \quad \text{for } l^2 + m^2 + n^2 \geq 1 \quad (6)$$

Thus, eq 5 can be split into a condition stating that segments cannot overlap

$$g(0, 0, 0) = 0 \quad (7)$$

and into

$$c(l, m, n) = 0 \quad \text{for } l^2 + m^2 + n^2 \geq 1 \quad (8)$$

Equations 2 (without indices *ij*), 3, 7, and 8 form a closed set of equations that can be solved for $h(l, m, n)$ if $\omega(l, m, n)$ and η_m are known.

Finally, an overall two-particle distribution $G(l, m, n)$, consisting of an intramolecular and an intermolecular part, can be defined according to

$$\eta_m G(l, m, n) = \omega(l, m, n) + \eta_m g(l, m, n) \quad (9)$$

where $\eta_m G(l, m, n)$ denotes the number of particles at position (l, m, n) from a chosen particle. This quantity is directly related to the EoS behavior of the athermal polymeric lattice fluid (see section 2.4).

2.2. Solution Method. Solution of eqs 2−8 is convenient in Fourier space.[53] In Fourier space eq 3 reads

$$\hat{h}(u, v, w) = \hat{\omega}(u, v, w) \hat{c}(u, v, w)(\hat{\omega}(u, v, w) + \eta_m \hat{h}(u, v, w)) \quad (10)$$

with the Fourier transform defined by

$$\hat{f}(u, v, w) = \sum_{l,m,n} f(l, m, n) \cos lu \cos mv \cos nw \quad (11)$$

and inverse

$$f(l, m, n) = \left(\frac{1}{2\pi}\right)^3 \int_{-\pi}^{\pi} \int_{-\pi}^{\pi} \int_{-\pi}^{\pi} \hat{f}(u, v, w) \cos lu \cos mv \cos nw \, du \, dv \, dw \quad (12)$$

Note that this transform only applies for symmetric functions, $f(l, m, n) = f(\pm l, \pm m, \pm n)$.

Writing eq 10 explicitly in terms of $\hat{h}(u, v, w)$, applying the inverse transformation eq 12, substituting $\hat{c}(u, v, w)$ (see eqs 8 and 11), and combining with the nonoverlap condition $h(0, 0, 0) = -1$ (eq 7) results in a single equation for the only unknown c_0:

$$-1 = \left(\frac{1}{2\pi}\right)^3 \int_{-\pi}^{\pi} \int_{-\pi}^{\pi} \int_{-\pi}^{\pi} \frac{\hat{\omega}^2(u, v, w) c_0}{1 - \eta_m \hat{\omega}(u, v, w) c_0} \, du \, dv \, dw \quad (13)$$

Equation 13 can be solved efficiently for c_0 with a Newton−Raphson scheme combined with a 3D-quadrature routine if η_m and $\hat{\omega}(u, v, w)$ are set in advance (see next subsection). Once c_0 is found, we can obtain $h(l, m, n)$ from eq 12 for $f = h$ and $\hat{h}$ given by eq 10. Note that it only takes the solution of one equation in one unknown to determine the structural properties of athermal polymeric lattice fluids.

The solution becomes particularly easy in the case of an athermal monomeric fluid. We have $\hat{\omega}(u, v, w)$ and, from eq 13, c_0 is directly found to be $c_0 = -1/(1 - \eta_m)$. From eq 12 we then find $h(0, 0, 0) = -1$ and $h(l, m, n \neq 0, 0, 0) = 0$. This illustrates that all structural correlations disappear in case the particles of the monomeric lattice fluid occupy exactly one lattice site. This is in great contrast to the monomeric continuum fluid, where packing effects determine the (complicated) solution of $h(l, m, n)$.[28,29] Thus, the lattice model presented here allows to study the influence of chain connectivity on the structural correlations without the liquidlike ordering effects that are observed in continuum space models at higher packing fractions.

2.3. The Intramolecular Distribution Function. In this subsection, the intramolecular distribution functions $\omega(l, m, n)$ used in the calculations are presented. Generally, $\omega(l, m, n)$ is not known for flexible molecules because the surrounding medium influences the conformation of each molecule: there is an intrinsic coupling of $\omega(l, m, n)$ and $g(l, m, n)$, and contrary to rigid molecules, $\omega(l, m, n)$ is not obtainable separately. It is thus impossible to use it as an input function for the calculation of $g(l, m, n)$ in the RISM equation. Curro and Schweizer[39] have solved this problem by invoking Flory's ideality hypothesis,[48] which states that for dense polymer melts there is a balance between inter- and intramolecular excluded volume interactions, implying that the mean squared end to end distance $\langle R^2 \rangle$ scales linearly with the number of covalent bonds, $s - 1$, in the chain. Such scaling behavior is also observed for the random flight (RF) model[56] and the nonreversal random walk model (NRRW). Therefore, Curro and Schweizer argue that such chain models are good candidates for the intramolecular distribution function in the polymer−RISM theory. In this paper we have tested both. An alternative solution to deal with the

intrinsic coupling of $g(l, m, n)$ and $\omega(l, m, n)$ has been presented in the form of a fully self-consistent scheme.[45−47]

The Fourier transform of the RF intramolecular two-particle distribution can be shown to be given by[58]

$$\hat{\omega}_{RF}(u, v, w) = \frac{1 - \hat{\tau}^2 - \frac{2}{s}\hat{\tau} + \frac{2}{s}\hat{\tau}^{s+1}}{(1 - \hat{\tau})^2} \qquad (14)$$

where $\hat{\tau} = {}^1/_3(\cos u + \cos v + \cos w)$ is the Fourier transformed 1-jump probability. (For a RF on a cubic lattice, $\tau(l, m, n) = 1/6$ if $l^2 + m^2 + n^2 = 1$ and zero otherwise.) Equation 14 is of the same form as the Gaussian distribution considered in continuum systems.[57,59]

Apart from the RF model we have also investigated the NRRW model. In the NRRW model, direct backfolding of the chains, such that segments $i - 1$ and $i + 1$ overlap, is forbidden. This leads to an expansion of the chains compared to the RF case: the RF mean squared end-to-end distance is approximately ${}^2/_3$ of the NRRW end-to-end distance (for infinitely long chains the factor ${}^2/_3$ is exact). The method for obtaining the NRRW-intramolecular distribution is outlined in Appendix A.

Finally, we have also used the intramolecular distribution obtained from the Monte Carlo simulations, presented in section 3, as an input in the discretized RISM-equation, eq 3. This $\omega(l, m, n)$ does not invoke the ideality assumption, contrary to the intramolecular distributions of the RF and NRRW chains, and accounts for excluded volume contributions.

2.4. Equation of State. As mentioned in the introduction, we here investigate the compressibility route to the equation of state, despite its problems when combined with the PRISM theory for continuum fluids. It is known that the PRISM equation does not yield the correct limiting low density behavior, and this will have its consequence for the integration to be conducted in eq 16. Other possible routes to the equation of state are, e.g. the energy equation, the virial equation, and the wall equation of state.[50] However, whereas the compressibility route results in an underestimation of the compressibility factor (a point we wish to address in this paper), the virial equation of state results in an overestimation.[50] For continuum fluids, the wall equation of state produced results which were believed to be nearest to the true behavior.[50] However, in a lattice study it was also shown that the wall equation of state was by no means in good agreement with MC simulation data,[55] which was a good reason for us to explore the compressibility route. Irrespective of which route is selected, it must be anticipated that the calculation of the equation of state with integral equation theory meets with great difficulties. The general relation of the isothermal compressibility $\kappa_T = 1/\eta_m(\partial\eta_m/\partial p)_{T,V}$ to the density fluctuations[60] is given for lattice systems by[54,58]

$$\frac{k_B T}{v_0}\kappa_T = \sum_{l,m,n}(G(l, m, n) - 1) \qquad (15)$$

in which $G(l, m, n)$ is the total two-particle distribution given by eq 9. Note from eq 15 that the compressibility is determined by the overall two-particle distribution $G(l, m, n)$ and not by the intermolecular distribution $g(l, m, n)$ alone.

Integration of eq 15 and substitution of eq 10 gives

$$\frac{pv_0}{k_B T}\int_0^{\eta_m}\left(\frac{1}{\hat{\omega}(0, 0, 0)} - \eta'_m\hat{c}(0, 0, 0)\right)d\eta'_m \qquad (16)$$

Equation 16 is the compressibility EoS. Note that $\hat{\omega}(0, 0, 0) = \sum_{l,m,n}\omega(l, m, n) = s$ effectively counts the segments that belong to a chain. Baxter has analytically performed the integration over the density in the compressibility equation for monomeric continuum fluids within the PY closure.[61] His expression can be modified for 3D athermal lattice polymers assuming a density independent intramolecular correlation function. Equation 16 is then given by (see Appendix B)

$$\frac{pv_0}{k_B T} = \frac{\eta_m}{s} - \eta_m{}^2 c(0, 0, 0) + \left(\frac{1}{2\pi}\right)^3\int_{-\pi}^{\pi}\int_{-\pi}^{\pi}\int_{-\pi}^{\pi}(\eta_m\hat{\omega}(u, v, w)\hat{c}(u, v, w) + \ln(1 - \eta_m\hat{\omega}(u, v, w)\hat{c}(u, v, w)))\,du\,dv\,dw \qquad (17)$$

In case of a monomeric system, eq 17 reduces to $pv_0/k_BT = -\ln(1 - \eta_m)$. This equation is exact, in contrast to its continuum analog, as can be verified via exact enumeration. Honnell, Hall, and Dickman have presented an EoS for continuum polymeric fluids that was derived via the pressure route.[62] This equation is not valid for lattice systems and it is not studied here. A lattice analog of the pressure equation that uses the depletion profiles of the polymeric fluid at a repulsive wall does however exist[49] and is presented elsewhere.[55]

3. Monte Carlo Simulation

The simulation method used to obtain the two-particle distributions, $g(l, m, n)$ and $\omega(l, m, n)$, and the equation of state for $s = 2$, $s = 16$, and $s = 30$ athermal chain fluids is of NpT type and is described in detail elsewhere.[18] It consists of condensing a polymer slab against a wall in a rectangular section of the cubic lattice with 50 sites in the l -direction, perpendicular to the wall, and 22 sites in the other two directions. Periodic boundary conditions are used in m and n directions. A finite pressure is exerted by fluctuating the total volume. The volume fluctuations are created by building/destroying a solid piston site-by-site with respect to the solid wall that is located at $l = 0$.

The configuration space is sampled by moving the polymer molecules on the lattice with reptation moves.[63] A volume fluctuation move was applied every 200 reptations. Up to 1.2×10^9 reptation moves were used, from which the first $(0.4-0.6) \times 10^9$ were used only for equilibration of each state. Averaging of thermodynamic properties took place every 5000 reptations. The particle distributions were only obtained from the last 0.1×10^9 moves. Averages of $g(l, m, n)$ and $\omega(l, m, n)$ were collected every 5000 reptations from a middle section of the polymer slab, at least 7 sites away from the solid wall and from the jagged edge of the piston. The $g(l, m, n)$ and $\omega(l, m, n)$ were only obtained for $r = (l^2 + m^2 + n^2)^{1/2} \le 4$. All runs were performed on a RISC IBM 6000 machine. The longest runs for the highest packing fractions took circa 30 h of CPU time.

4. Results and Discussion

In section 4.1 we compare the structural properties of the discretized polymer−RISM model to Monte Carlo data. In section 4.2 we compare its EoS properties to

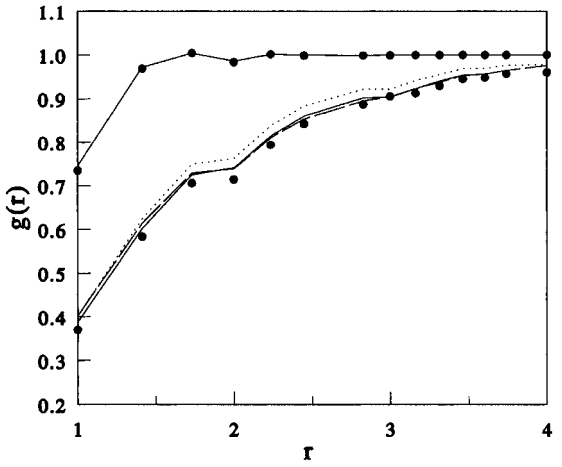

Figure 1. Intermolecular two-particle distribution in an athermal dimeric fluid at $\eta_m = 0.3014$ (upper symbols and lines) and an athermal 16-mer fluid at $\eta_m = 0.3198$ (lower symbols and lines). Symbols are obtained from MC simulation and lines from the discretized polymer−RISM theory. For the 16-mer fluid three lines are shown: the dotted line is obtained for random flight chains, the full line is obtained for NRRW chains, and the dashed line is calculated with the intramolecular distribution function obtained from the simulations.

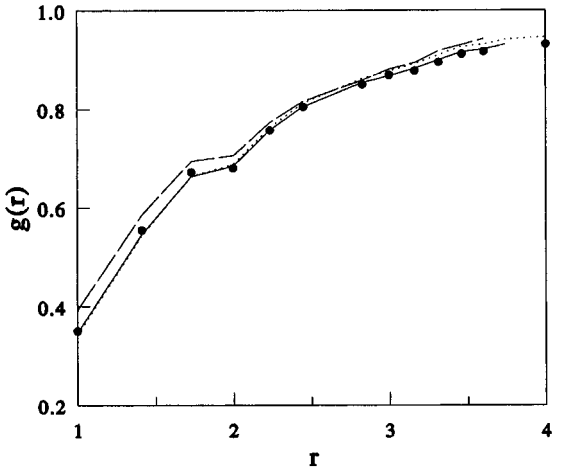

Figure 2. Intermolecular two-particle distribution in an athermal 30-mer fluid at $\eta_m = 0.3867$. Symbols are obtained from MC simulation; lines are obtained from theory. The dotted line is obtained for random flight chains and the full line for NRRW-chains, and the dashed line is calculated with the intramolecular distribution function obtained from the simulations.

NpT-simulation data and to predictions of a compressible version of the Huggins theory.[12,18] Both the simulation method and the compressible lattice Huggins theory have been considered previously in ref 18.

4.1. Structural Correlations. In Figures 1 and 2 the intermolecular distribution $g(l, m, n)$ of noninteracting dimers and 16-mers (Figure 1), and 30-mer fluids (Figure 2) at the indicated segment packing fractions are shown as a function of segment−segment separation distance. We have plotted $g(l, m, n)$ as $g(r)$ with $r = (l^2+m^2+n^2)^{1/2}$. This is not fully correct, as $g(l, m, n)$ is not fully isotropic; e.g., $g(2, 2, 1)$ and $g(3, 0, 0)$ have slightly different values. Plotting as $g = g(r)$ is a necessity, however, in making 2D plots, and the reduction of information is only marginal because $g(2, 2, 1) \approx g(3, 0, 0)$. We have obtained $g(3)$ by numerical averaging of $g(2, 2, 1)$ and $g(3, 0, 0)$. The simulation data in the figures are denoted by symbols and the results of the calculations by the lines. The use of lines does not mean that the results of the calculations for $g(r)$ are continuous with r, but this is done is merely to distinguish between theory and simulation. The error bars on the simulations shown in the figures are smaller than the size of the symbols and are therefore omitted.

In Figure 1 (upper symbols and line) it is seen that the polymer−RISM equation is able to accurately reproduce the intermolecular two-particle distribution of a dimeric lattice fluid with the intramolecular distribution function eq 4 given by

$$\omega_{11}(0, 0, 0) = 1$$

$$\omega_{11}(l, m, n) = 0 \quad \text{for } l^2 + m^2 + n^2 \geq 1$$

$$\omega_{12}(l, m, n) = \frac{1}{6} \quad \text{for } l^2 + m^2 + n^2 = 1$$

$$\omega_{12}(l, m, n) = 0 \quad \text{otherwise} \qquad (18)$$

and $\omega_{ij}(l, m, n) = \omega_{ji}(l, m, n)$. Note that for dimeric lattice fluids, eq 18 is exact, as is Curro and Schweizer's equivalence of segments that lead to eq 3. The decrease of $g(r)$ for $r = 1$ shown by the upper curve in the figure is due to the fact that one of the six nearest neighbors of each dimer segment is taken by the other segment of the dimer (chemical bonding). This leaves less room for particles (segments) belonging to other molecules and results in a lower probability, $\eta_m g(r)$, of encountering particles belonging to different molecules on the nearest neighbor positions. This decrease of $g(r)$ for smaller r is called the correlation hole effect.[39]

In Figures 1 and 2, it is seen that the correlation hole is deeper in polymeric fluids when compared to a dimeric fluid at roughly the same packing fraction. This is because in a polymeric fluid most segments are covalently bonded to two other segments and not to one, as is the case for the dimeric fluid. It is also seen that the correlation hole extends over larger interparticle distances, which is because the average separation distance between the chain ends is proportional to $(s - 1)^{1/2}$. Notice from Figures 1 and 2 that the intermolecular two-particle distribution, $g(r)$, does not scale monotonically with r: cubic lattice fluids are not isotropic. Two particles at distance (2, 0, 0) are relatively strongly correlated, because there are only two nearest neighbor contacts for which correlation loss occurs on the shortest path between the particles. For two particles at distance (1, 1, 1), the minimum number of nearest neighbor contacts is three, although the particles are closer than the particles at (2, 0, 0). It is only because there are more shortest distance paths between two particles at (1, 1, 1), while there is only one between the particles at (2, 0, 0), that the particles at (1, 1, 1) are not always more weakly correlated than the particles at (2, 0, 0).

For the polymeric fluids in Figures 1 and 2 we have tested several intramolecular segment−segment distributions, $\omega(l, m, n)$, on their ability to reproduce $g(l, m, n)$ via the polymer−RISM equation, eq 3. Note first that the results for $g(l, m, n)$ are satisfying, when compared to the simulations (symbols), for all cases tested. The dotted lines in both figures are obtained for the random flight intramolecular distribution of eq 14. Note that this distribution is a little more accurate for the $s = 30$-mer, indicating that the polymer−RISM equation is more accurate for longer chains. This is obviously due to the equivalence of segments approximation underly-

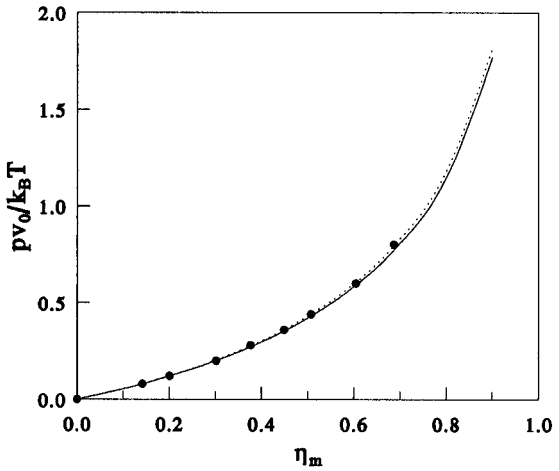

Figure 3. Equation of state of the athermal dimeric lattice fluid. The symbols indicate simulated states, and the full line indicates the EoS obtained from the discretized polymer−RISM theory with eq 17. The dotted line is obtained from the compressible Huggins EoS, eq 19.

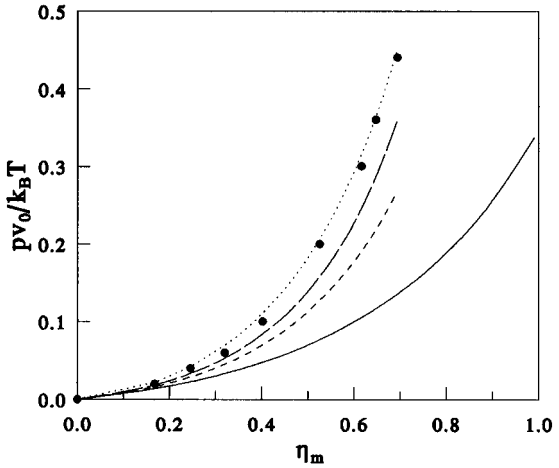

Figure 4. EoS of athermal $s = 16$-mers. Symbols indicate simulation results, and the lines are obtained for the random flight (full line), the NRRW (short dash) and Monte Carlo (long dash) intramolecular two-particle distributions. The dotted line is obtained from eq 19.

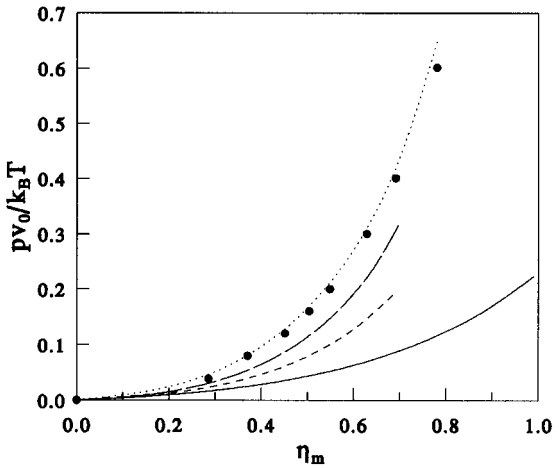

Figure 5. EoS as in Figure 4 but for $s = 30$-mers.

ing eq 3. The NRRW-chain model (Appendix A) is also shown in Figures 1 and 2 by the full line. A little improvement, when compared to the RF model, especially for $s = 16$, is observed in both figures, but the influence of an improved intramolecular distribution clearly is marginal. Finally, the results obtained by inserting the $\omega(l, m, n)$, monitored from the MC simulations, in eq 3 are also shown by the long dashed lines. In the case of $s = 16$ virtually no improvement is seen when compared to the NRRW-chain, and for $s = 30$ we observe a less accurate description of $g(l, m, n)$, when compared to the RF- or NRRW-chain model. This is due to the fact that only $\omega(l, m, n)$ for $r = (l^2 + m^2 + n^2)^{1/2} \leq 4$ was extracted from the simulations and fed into the polymer−RISM equation. The tail-contribution of $\omega(l, m, n)$ for $r > 4$ was simply set to zero. This procedure, to which we have resorted to reduce the CPU-times needed in the simulations, is obviously not correct, but does illustrate that the values of $\omega(l, m, n)$ for the small separation distances $r \leq 4$ largely determine the behavior of $g(l, m, n)$: in both figures we still get reasonable results if we use $\omega(l, m, n)$ for $r \leq 4$ only. At other packing fractions we have found results similar to those shown in Figures 1 and 2. It should be realized that it takes the solution of only one equation in the unknown $c(0, 0, 0)$ to calculate the $g(l, m, n)$'s shown in the figures.

4.2. Equation of State. Figures 3−5 show the EoS-results for athermal dimers (Figure 3), 16-mers (Figure 4), and 30-mers (Figure 5). From the MC-points in the figures it is seen that a fluid consisting of longer chains is more easily pressurized,[64] although the chain length dependence decreases rapidly with chain length.

From Figure 3 it is seen that the compressibility-EoS, eq 17, for dimers (full line) accurately captures the simulation results (symbols), although the dotted line is still marginally better. This dotted line is calculated from the Huggins approximation for a compressible lattice fluid. It is given by[10,12,18]

$$\frac{pv_0}{\eta k_B T} = \frac{s-1}{c}\frac{\ln(1-c\eta_m)}{\eta_m} - \frac{s\ln(1-\eta_m)}{\eta_m} \qquad (19)$$

with

$$c = \frac{2}{6}\left(1 - \frac{1}{s}\right) \qquad (20)$$

In Figures 4 and 5 the EoS of respectively $s = 16$-mers and $s = 30$-mers are shown. It is seen that the EoS calculated with eq 19 (dotted line) is quite accurate when compared to the MC-data. The other curves shown in the figures are based on the compressibility-EoS, eq 17, for respectively the random flight intramolecular distribution (full curve), the NRRW intramolecular distribution of Appendix A (short dash), and the intramolecular distribution function extracted from MC simulations (long dash). The intramolecular distribution function extracted from the simulations was again only considered for $r \leq 4$ lattice spacings and set to zero for $r > 4$. It is seen from the figures for $s = 16$ and $s = 30$ that the Random Flight chains produce an equation that is far off the MC data. Subsequent improvements are obtained by using the intramolecular distribution of a NRRW chain and the $\omega(l, m, n)$ obtained from the simulations. In particular for the latter intramolecular distribution function the predicted equation of state is in acceptable agreement with the MC simulation data although the classical Huggins EoS performs even better.

The compressibility EoS for monomers is exact and the compressibility EoS for dimers is very accurate. Therefore, the results shown in Figures 4 and 5 must be caused by the inexactitude of the intramolecular distributions of flexible chains and not by an intrinsic

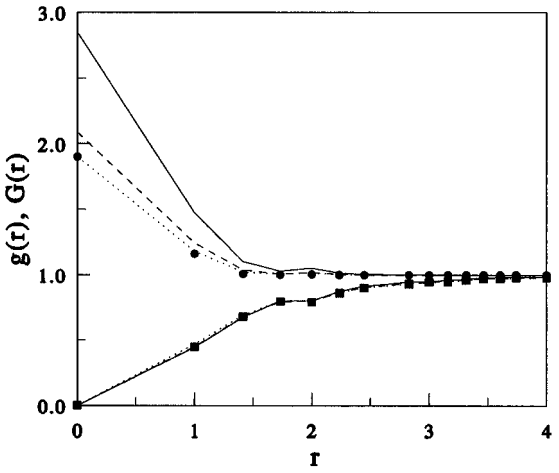

Figure 6. Total- and intermolecular two-particle distribution of an athermal $s = 16$-mer at $\eta_m = 0.526$. The symbols indicate simulation results for $G(l, m, n)$ (●) and $g(l, m, n)$ (■). The lines result from the calculations. The upper curves indicate the total distributions, and the lower curves, the intermolecular distributions. Results are obtained for a random flight chain (full line), a NRRW chain (dashed line), and the intramolecular distribution obtained from MC simulations (dotted line).

unsuitability of the compressibility route to produce an accurate EoS. This is understood as follows. Due to the approximate incorporation of excluded volume, conformations in which segments of the same molecule overlap contribute to $\omega(l, m, n)$. Consequently, the fluid can more easily be compressed than a fluid in which the segments never show any overlap. As a result, the dependence of the pressure on η_m is not strong enough. In Figures 4 and 5 it is seen that the $\omega(l, m, n)$ extracted from the MC simulations produces the best results. This is simply because it most accurately incorporates the chain-excluded volume. An even better EoS could have been obtained if $\omega(l, m, n)$ had been extracted up to larger distances from the simulations, but such a procedure is computationally intensive. Apart from the (partial) neglect of excluded volume in the intramolecular distribution function, we also neglect its density dependence when integrating eq 16 (see Appendix B) (for low density systems the chains look like self-avoiding random walks; at higher densities they behave as self-overlapping random walks). This, also, is a reason for the poorer behavior of the compressibility EoS for flexible chains when compared to monomeric and dimeric fluids.

The consequence for the EoS of an incorrect $\omega(l, m, n)$, i.e., an $\omega(l, m, n)$ which partially neglects excluded volume interactions and is density independent, can be clearly shown with help of eq 15. It shows that the compressibility, κ_T (and thus the pressure via eq 16), is determined by the total two-particle distribution $G(l, m, n)$, and not by the intermolecular distribution $g(l, m, n)$ alone. Thus, although the $\omega(l, m, n)$'s studied in this paper all provide a fairly accurate description of the intermolecular segmental distributions $g(l, m, n)$, this does not mean that they also produce an accurate compressibility EoS. This is illustrated in Figure 6.

It displays the intermolecular (lower symbols and curves) and the total two-particle distribution (upper symbols and curves) of a $s = 16$ -mer for our three intramolecular distributions. It is clearly shown that the $g(l, m, n)$'s, calculated from eq 3, are not very sensitive to the exact nature of $\omega(l, m, n)$, in contrast with the total two-particle distribution $G(l, m, n)$, which is highly sensitive to $\omega(l, m, n)$. Unfortunately, it is $G(l, m, n)$ and not $g(l, m, n)$ that determines the EoS behavior. Therefore, the EoS also shows a strong sensitivity on $\omega(l, m, n)$. The overestimation at small distances of $G(l, m, n)$ for the RF (full line) and NRRW fluid (dashed line) are caused by the approximate incorporation of excluded volume in $\omega_{RF}(l, m, n)$ and $\omega_{NRRW}(l, m, n)$: segmental overlaps produce at small distances values too large for the ω's and thus for the G's. Clearly, the best $G(l, m, n)$ is obtained with the $\omega(l, m, n)$ taken from the simulations (dotted line), but even this $\omega(l, m, n)$ is not accurate enough to produce an EoS comparable to the compressible Huggins EoS. More accurate results can only be obtained by explicitly accounting for the density dependence of $\omega(l, m, n)$, and by properly accounting for the excluded volume and long-range contributions of $\omega(l, m, n)$. The excluded volume problem can be studied employing an Ornstein−Zernike integro−difference equation suggested by Curro, Blatz, and Pings.[65] Combining the intramolecular correlation function, derived from this theory, with the PRISM equation yields good results for the structural correlations and the EoS of athermal polymeric lattice fluids.[66] The density dependence must be addressed using a self-consistent scheme,[45−47] in which an intrinsic coupling of $\omega(l, m, n)$ and $g(l, m, n)$ is established, although such a scheme will only produce an accurate EoS if both $\omega(l, m, n)$ and $g(l, m, n)$ are precisely obtained (i.e., if $\omega(l, m, n)$ shows the correct excluded volume behavior and if both $\omega(l, m, n)$ and $g(l, m, n)$ display the correct density dependence). In conclusion, one may expect that the computation of the equation of state and also other thermodynamic properties employing integral equation theories always will meet considerable difficulties.

5. Conclusions

Polymer−RISM theory[39] was used to study a cubic lattice model of an athermal polymer fluid. Both the structural and the EoS properties of the fluid were obtained. The results for the structural correlations and the equation of state have been compared to NpT Monte Carlo simulation results. The EoS properties are also compared to a classic EoS based on the Huggins approximation. The intermolecular two-particle distribution compares very well with simulation results, while the EoS behavior is reasonable. The EoS obtained thus far is worse than the EoS obtained on the basis of the Huggins approximation for the same model system. An important reason for this failure of the polymer−RISM approach, i.e. the complete (RF) or partial (NRRW) absence of excluded volume in the intramolecular distribution functions, has been clarified. This was particularly easy due to the use of a lattice model for which liquidlike packing effects are absent. Note, however, that the compressibility EoS for continuum fluids obtained with the polymer−RISM theory[39] suffers from the same failure (see e.g., Figure 2 of ref 64). We, therefore, think that lattice models may be of help in understanding/improving results obtained with the continuum version of the polymer−RISM equation.

Appendix A. NRRW−Chain Intramolecular Distribution

The NRRW-intramolecular distribution has been calculated in real space, after which it was Fourier transformed via eq 11 into the form $\hat{\omega}_{NRRW}(u, v, w)$ required by eq 13.

$\omega_{\mathrm{NRRW}}(l, m, n)$ was obtained as follows. From eq 4 it is seen that an s-mer intramolecular distribution consists of two flights of $s-1$ jumps (ω_{1s} and ω_{s1}), four $s-2$ flights, six $s-3$ flights, etc. Thus

$$\omega(l, m, n) = 1 + \frac{2}{s}\sum_{i=1}^{s-1}(s - \mathrm{i})W_i(l, m, n) \qquad \text{(A1)}$$

where $W_i(l, m, n)$ is the probability that a jump consisting of i-steps starting at (0, 0, 0) ends at (l, m, n). The 1 accounts for the self-correlation of segments (the ω_{ii} contribution in eq 4).

Now, in order to calculate the real space jump probabilities $W_i(l, m, n)$ of a nonreversal random walk, we need to separate the $W_i(l, m, n)$'s into six parts

$$\begin{aligned} W_i(l, m, n) = {} & W_i((l, m, n); (l+1, m, n)) + \\ & W_i((l, m, n); (l-1, m, n)) + W_i((l, m, n); (l, m+1, n)) + \\ & W_i((l, m, n); (l, m-1, n)) + W_i((l, m, n); (l, m, n+1)) + \\ & W_i((l, m, n); (l, m, n-1)) \end{aligned} \qquad \text{(A2)}$$

The two arguments of the jump probabilities on the right-hand side of this equation denote the positions of the last two segments, $i+1$ and i, after i jumps. Each of the jump probabilities on the rhs can then be expressed in $i-1$ jump probabilities; e.g., for $W_i((l, m, n); (l-l, m, n))$, we have

$$\begin{aligned} W_i((l, m, n); (l-1, m, n)) = {} & \tau W_{i-1}((l-1, m, n); (l-2, m, n)) + \tau W_{i-1}((l-1, m, n); (l-1, m+1, n)) + \\ & \tau W_{i-1}((l-1, m, n); (l-1, m-1, n)) + \\ & \tau W_{i-1}((l-1, m, n); (l-1, m, n+1)) + \\ & \tau W_{i-1}((l-1, m, n); (l-1, m, n-1)) \end{aligned} \qquad \text{(A3)}$$

with $\tau = \tau(1, 0, 0)$ being the 1-jump probability. The arguments of W_{i-1} again denote the coordinates of the last two segments, i and $i-1$, after $i-1$ jumps. In eq A3 we have left out the prohibited jump $\tau(1, 0, 0)W_{i-1}((l-1, m, n); (l, m, n))$ which corresponds to direct backfolding. The single jump probability τ equals $^1/_5$ due to the absence of direct back folding.

From $W_1((1, 0, 0); (0, 0, 0)) = {}^1/_6$ (and zero otherwise), one can immediately evaluate the $W_2((l, m, n); (l', m', n'))$ with help of eq A3. Further recursive use of this equation leads to $W_i((l, m, n); (l', m', n'))$. The $W_i(l, m, n)$ can then be obtained via eq A2, and finally, $\omega_{NRRW}(l, m, n)$ follows via eq A1. The method becomes increasingly time consuming for long chains but the chains considered here (up to $s = 30$) could easily be studied in this way.

Appendix B. Compressibility EoS for Athermal Lattice Polymers

In this appendix we apply Baxter's integration method[61] to the compressibility EoS for athermal lattice polymers.

We start from the definition (see ref 30)

$$\begin{aligned} I_{\mathrm{RISM}} = {} & \eta_{\mathrm{m}}{}^2 c(0, 0, 0) + \\ & \left(\frac{1}{2\pi}\right)^3 \int_{-\pi}^{\pi}\int_{-\pi}^{\pi}\int_{-\pi}^{\pi} (\eta_{\mathrm{m}}\hat{\omega}(u, v, w)\hat{c}(u, v, w) + \\ & \ln(1 - \eta_{\mathrm{m}}\hat{\omega}(u, v, w)\hat{c}(u, v, w)))\, \mathrm{d}u\, \mathrm{d}v\, \mathrm{d}w \end{aligned} \qquad \text{(B1)}$$

Note that for athermal lattice polymers $\hat{c}(u, v, w) = c(0, 0, 0) = c_0$. Differentiating I_{RISM} with respect to c_0 gives

$$\frac{\partial I_{\mathrm{RISM}}}{\partial c_0} = \eta_{\mathrm{m}}{}^2(1 + h(0, 0, 0)) = 0 \qquad \text{(B2)}$$

We then define P, which, as will be shown, can be identified with the compressibility pressure p, as

$$\begin{aligned} \frac{Pv_0}{k_{\mathrm{B}}T} = {} & \frac{\eta_{\mathrm{m}}}{s} - \eta_{\mathrm{m}}{}^2 c(0, 0, 0) + \\ & \left(\frac{1}{2\pi}\right)^3 \int_{-\pi}^{\pi}\int_{-\pi}^{\pi}\int_{-\pi}^{\pi} (\eta_{\mathrm{m}}\hat{\omega}(u, v, w)\hat{c}(u, v, w) + \\ & \ln(1 - \eta_{\mathrm{m}}\hat{\omega}(u, v, w)\hat{c}(u, v, w)))\, \mathrm{d}u\, \mathrm{d}v\, \mathrm{d}w \end{aligned} \qquad \text{(B3)}$$

differentiating $Pv_0/k_{\mathrm{B}}T$ with respect to η_{m} gives

$$\begin{aligned} \frac{\partial(Pv_0/k_{\mathrm{B}}T)}{\partial\eta_{\mathrm{m}}} = {} & 1/s - 2\eta_{\mathrm{m}}c_0 - \eta_{\mathrm{m}}{}^2\partial c_0/\partial\eta_{\mathrm{m}} + \\ & \left(\frac{1}{2\pi}\right)^3 \int_{-\pi}^{\pi}\int_{-\pi}^{\pi}\int_{-\pi}^{\pi} (\hat{\omega}(u, v, w) - \\ & \hat{\omega}(u, v, w)/(1 - \eta_{\mathrm{m}}\hat{\omega}(u, v, w)c_0))c_0\, \mathrm{d}u\, \mathrm{d}v\, \mathrm{d}w + \\ & \left(\frac{1}{2\pi}\right)^3 \int_{-\pi}^{\pi}\int_{-\pi}^{\pi}\int_{-\pi}^{\pi} (\eta_{\mathrm{m}}\hat{\omega}(u, v, w) - \\ & \eta_{\mathrm{m}}\hat{\omega}(u, v, w)/(1 - \eta_{\mathrm{m}}\hat{\omega}(u, v, w)c_0))\, \partial c_0/\partial\eta_{\mathrm{m}}\, \mathrm{d}u\, \mathrm{d}v\, \mathrm{d}w \end{aligned} \qquad \text{(B4)}$$

Substituting eq B2 in eq B4 then immediately leads to

$$\partial(Pv_0/k_{\mathrm{B}}T)/\partial\eta_{\mathrm{m}} = 1/s - \eta_{\mathrm{m}}c_0 \qquad \text{(B5)}$$

Integration with respect to η_{m} thus gives eq 16 if we identify P with the pressure p. We can thus set $P = p$ in eq B3, giving eq 17.

Note that in deriving eq 17 we have neglected the density dependence of $\omega(l, m, n)$ which is an approximation inherent in the standard polymer−RISM theory.[39]

References and Notes

(1) Prigogine, I. *The Molecular Theory of Solutions*; North-Holland Publishing Company: Amsterdam, 1957.
(2) Flory, P. J.; Orwoll, R. A.; Vrij, A. *J. Am. Chem. Soc.* **1964**, *86*, 3567.
(3) Sanchez, I. C.; Lacombe, R. U. *J. Phys. Chem.* **1976**, *80*, 2352.
(4) Kleintjens, L. A.; Koningsveld, R. J. *J. Electrochem. Soc.* **1980**, *121*, 2353.
(5) Simha, R.; Somcynsky, T. *Macromolecules* **1969**, *2*, 341.
(6) Dickman, R.; Hall, C. K. *J. Chem. Phys.* **1986**, *85*, 4108.
(7) Chiew, Y. C. *Mol. Phys.* **1990**, *70*, 129.
(8) Wertheim, M. S. *J. Chem. Phys.* **1987**, *87*, 7323.
(9) Schweizer, K. S.; Curro, J. G. *J. Chem. Phys.* **1988**, *89*, 3342.
(10) Guggenheim, E. A. *Mixtures*; Clarendon Press: Oxford, England, 1952.
(11) Flory, P. J. *J. Chem. Phys.* **1941**, *9*, 660.
(12) Huggins, M. L. *J. Chem. Phys.* **1941**, *9*, 440.
(13) Nies, E.; Stroeks, A. *Macromolecules* **1990**, *23*, 4088.
(14) Nies, E.; Xie, H. *Macromolecules* **1993**, *26*, 1683.
(15) Hill, T. L. *Statistical Mechanics*; McGraw-Hill Book Co.: New York, 1956.
(16) Hill, T. L. *An Introduction to Statistical Thermodynamics*; Addison-Wesley Publishing Co.: Reading, MA, 1960.
(17) Prigogine, I.; Defay, R. *Chemical Thermodynamics*; Longmans Green and Co.: London, 1954.
(18) Nies, E.; Cifra, P. *Macromolecules* **1994**, *27*, 6033.
(19) Mackie, A. D.; Panagiotopoulos, A. Z.; Kumar, S. K. *J. Chem. Phys.* **1995**, *102*, 1014.
(20) Sariban, A.; Binder, K. *Macromolecules* **1988**, *21*, 711.
(21) Müller, M.; Binder, K. *Comput. Phys. Commun.* **1994**, *84*, 173.
(22) Cifra, P.; Nies, E.; Broersma, J. *Macromolecules* **1996**, *29*, 6634.
(23) Honnell, K. G.; Hall, C. K. *J. Chem. Phys.* **1989**, *90*, 1841.
(24) Bawendi, M. G.; Freed, K. F. *J. Chem. Phys.* **1988**, *88*, 2741.
(25) Freed, K. F.; Dudowicz, J. *Macromolecules* **1996**, *29*, 625.

(26) Hansen, J. P.; McDonald, I. R. *Theory of Simple Liquids* 2nd ed.; Academic Press: London, 1986.
(27) Percus, J. K.; Yevick, G. J. *Phys. Rev.* **1958**, *110*, 1.
(28) Thiele, E. *J. Chem. Phys.* **1963**, *39*, 474.
(29) Wertheim, M. S. *Phys. Rev. Lett.* **1963**, *10*, 321.
(30) Chandler, D.; Andersen, H. C. *J. Chem. Phys.* **1972**, *57*, 1930.
(31) Wer842 Wertheim, M. S. *J. Stat. Phys.* **1986**, *42*, 477.
(32) McQuarrie, D. A. *Statistical Mechanics*; Harper and Row Publishers: New York, 1976.
(33) Weeks, J. D.; Chandler, D.; Andersen, H. C. *J. Chem. Phys.* **1971**, *54*, 5237.
(34) Chandler, D.; Weeks, J. D.; Andersen, H. C. *Science* **1983**, *220*, 787.
(35) Van Leeuwen, J. M. J.; Groeneveld, J.; De Boer, J. *Physica* **1959**, *25*, 792.
(36) Lebowitz, J. L.; Percus, J. K. *Phys. Rev.* **1966**, *144*, 251.
(37) Barker, J. A.; Henderson, D. *Rev. Mod. Phys.* **1976**, *48*, 587.
(38) Song, Y.; Mason, E. A. *J. Chem. Phys.* **1989**, *91*, 7840.
(39) Curro, J. G.; Schweizer, K. S. *Macromolecules* **1987**, *20*, 1928. For recent reviews see: Schweizer, K. S.; Curro, J. G. *Adv. Polym. Sci.* **1994**, *116*, 319. Schweizer, K. S.; Curro, J. G. *Adv. Chem. Phys.* **1996**, *98*, 1
(40) Chiew, Y. C. *Mol. Phys.* **1991**, *73*, 359.
(41) Wertheim, M. S. *J. Stat. Phys.* **1986**, *42*, 459.
(42) Yethiraj, A.; Schweizer, K. S. *J. Chem. Phys.* **1992**, *97*, 1455.
(43) Chiew, Y. C. *J. Chem. Phys.* **1990**, *93*, 5067.
(44) Chang, J.; Sandler, S. I. *J. Chem. Phys.* **1995**, *102*, 437.
(45) Schweizer, K. S.;Honnell, K. G.; Curro, J. G. *J. Chem. Phys.* **1992**, *96*, 3211.
(46) Melenkevitz, J.; Schweizer, K. S.; Curro, J. G. *Macromolecules* **1993**, *26*, 6190. Melenkevitz, J.; Curro, J. G.; Schweizer, K. S. *J. Chem. Phys.* **1993**, *99*, 5571.
(47) Grayce, C. J.; Schweizer, K. S. *J. Chem. Phys.* **1994**, *100*, 6846. Grayce, C. J.; Yethiraj, A.; Schweizer, K. S. *J. Chem. Phys.* **1994**, *100*, 6857.
(48) Flory, P. J. *J. Chem. Phys.* **1949**, *17*, 303.
(49) Dickman, R. *J. Chem. Phys.* **1987**, *87*, 2246.
(50) Yethiraj, A.; Curro, J. G.; Schweizer, K. S.; McCoy, J. D. *J. Chem. Phys.* **1993**, *98*, 1635. Appropriate references to the different equation of states routes are cited in this paper.
(51) Lipson, J. E. G. *J. Chem. Phys.* **1992**, *96*, 1418.
(52) Sevian, H. M.; Brazhnik, P. K.; Lipson, J. E. G. *J. Chem. Phys.* **1993**, *99*, 4112.
(53) Jancovici, B. *Physica* **1965**, *31*, 1017.
(54) Stell, G. *Phys. Rev.* **1969**, **184**, 135.
(55) Janssen, R. H. C.; Nies, E.; Cifra, P. *Langmuir* **1997**, *13*, 2784.
(56) Chandrasekhar, S. *Rev. Mod. Phys.* **1943**, *15*, 1.
(57) Curro, J. G.; Schweizer, K. S. *J. Chem. Phys.* **1987**, *87*, 1842.
(58) Janssen, R. H. C. Structure and Thermodynamics of Lattice Polymers in Bulk and at Interfaces. Ph.D. Thesis, Eindhoven University of Technology, Eindhoven, The Netherlands, 1996.
(59) Koyama, R. *J. Phys. Soc. Jpn.* **1973**, *34*, 1029.
(60) Kirkwood, J. G.; Buff, F. P. *J. Chem. Phys.* **1951**, *19*, 774.
(61) Baxter, R. J. *J. Chem. Phys.* **1967**, *47*, 4855.
(62) Honnell, K. G.; Hall, C. K.; Dickman, R. *J. Chem. Phys.* **1987**, *87*, 664.
(63) Wall, F. T.; Mandel, F. *J. Chem. Phys.* **1975**, *63*, 4592.
(64) Gao, J.; Weiner, J. H. *J. Chem. Phys.* **1989**, *91*, 3168.
(65) Curro, J. G.; Blatz, P. J.; Pings, C. J. *J. Chem. Phys.* **1969**, *50*, 2199.
(66) Wang, S.; Nies, E. To be published.

MA961386U